



HAL
open science

Fault Tolerance Analysis of Five-Level Neutral-Point-Clamped Inverters under Clamping Diode Open-Circuit Failure

Sajjad Ahmadi, Philippe Poure, Shahrokh Saadate, Davood Arab Khaburi

► **To cite this version:**

Sajjad Ahmadi, Philippe Poure, Shahrokh Saadate, Davood Arab Khaburi. Fault Tolerance Analysis of Five-Level Neutral-Point-Clamped Inverters under Clamping Diode Open-Circuit Failure. *Electronics*, 2022, 11 (9), pp.1461. 10.3390/electronics11091461 . hal-03873531

HAL Id: hal-03873531

<https://hal.science/hal-03873531>

Submitted on 26 Nov 2022

HAL is a multi-disciplinary open access archive for the deposit and dissemination of scientific research documents, whether they are published or not. The documents may come from teaching and research institutions in France or abroad, or from public or private research centers.



L'archive ouverte pluridisciplinaire **HAL**, est destinée au dépôt et à la diffusion de documents scientifiques de niveau recherche, publiés ou non, émanant des établissements d'enseignement et de recherche français ou étrangers, des laboratoires publics ou privés.



Distributed under a Creative Commons Attribution 4.0 International License

Article

Fault Tolerance Analysis of Five-Level Neutral-Point-Clamped Inverters under Clamping Diode Open-Circuit Failure

Sajjad Ahmadi ¹, Philippe Poure ^{2,*} , Shahrokh Saadate ¹ and Davood Arab Khaburi ³ 

¹ GREEN, Université de Lorraine, F-54500 Nancy, France; sajjad.ahmadi@univ-lorraine.fr (S.A.); shahrokh.saadate@univ-lorraine.fr (S.S.)

² CNRS, IJL, Université de Lorraine, F-54500 Nancy, France

³ The Center of Excellence for Power Systems Automation and Operation, Department of Electrical Engineering, Iran University of Science and Technology, Tehran 1311416846, Iran; khaburi@iust.ac.ir

* Correspondence: philippe.poure@univ-lorraine.fr

Abstract: Multilevel inverters are increasingly used in industrial applications in which service continuity is crucial. This paper presents an original approach to ensure the fault-tolerant operation of neutral-point-clamped (NPC) inverters in the case of an open-circuit fault event in a clamping diode, which is rarely investigated in the conducted research work. The proposed fault-tolerant strategy meets the following criteria: restoring rated output voltage and current during post-fault operation, realizing fault-tolerant operation without additional components, maintaining rated total harmonic distortion (THD) during fault-tolerant operation, and fast transition between faulty operation and remedial operation. In the proposed approach, prior to applying the appropriate remedial action, identification of the defective clamping diode is required. In this respect, a very fast and simple logic-based fault diagnosis is presented whose implementation does not need any additional components and external circuit. Moreover, it does not require any component modeling and complicated calculations. The proposed strategy is validated by simulation and experimentation.

Keywords: fault tolerance analysis; neutral-point-clamped (NPC) inverter; clamping diode; open-circuit failure



Citation: Ahmadi, S.; Poure, P.; Saadate, S.; Khaburi, D.A. Fault Tolerance Analysis of Five-Level Neutral-Point-Clamped Inverters under Clamping Diode Open-Circuit Failure. *Electronics* **2022**, *11*, 1461.

<https://doi.org/10.3390/electronics11091461>

Academic Editors: Hamed Habibi, Afef Fekih, Simani Silvio and Amirmehdi Yazdani

Received: 30 March 2022

Accepted: 28 April 2022

Published: 3 May 2022

Publisher's Note: MDPI stays neutral with regard to jurisdictional claims in published maps and institutional affiliations.



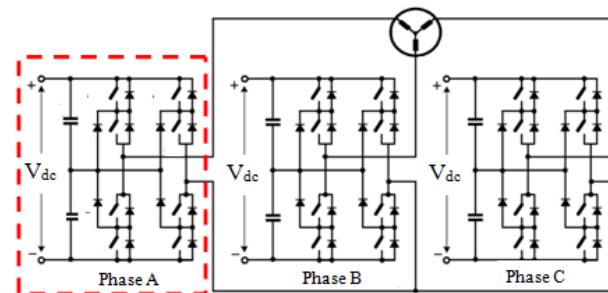
Copyright: © 2022 by the authors. Licensee MDPI, Basel, Switzerland. This article is an open access article distributed under the terms and conditions of the Creative Commons Attribution (CC BY) license (<https://creativecommons.org/licenses/by/4.0/>).

1. Introduction

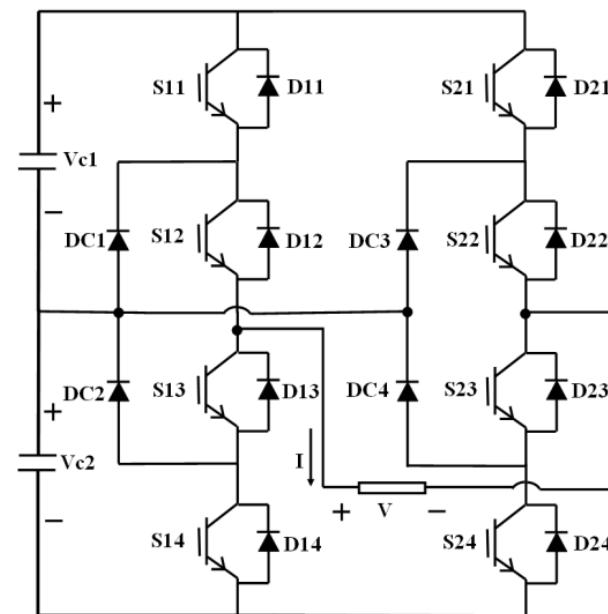
Multilevel inverters have been attracting wide attention in industry for some decades. These inverters have the following advantages: reduced total harmonic distortion, limited losses, reduced voltage transient, and smaller size of filter components. Thus, they provide major advantages, compared with two-level topologies [1,2]. Any transformers or flying capacitors are not used in neutral-point-clamped (NPC) topologies; thus, these circuits are increasingly used in industry. Nevertheless, in high-voltage applications, unequal voltage sharing increases [3]. To cope with this problem, NPC/H-bridge topology is preferred to classical NPC circuits. In order to constitute an NPC/H-bridge inverter from the topology of a three-phase three-level NPC inverter, each phase or leg of the classical NPC circuit is substituted by a single-phase five-level NPC module (see Figure 1a). Thus, as depicted in Figure 1a, each phase has its own DC link capacitors. Providing the independent DC voltage sources necessitates employing a transformer with a rectifier for each NPC module of the three-phase circuit, which complicates the structure of this type of inverter compared with the classical NPC inverter. This can be considered as a small disadvantage for this NPC/H-bridge inverter structure.

In NPC topology, clamping diodes have a key role to generate output voltage levels. In this circuit, solely the clamping diodes connect the inverter leg to the neutral point, whereas in the other topologies such as T-type or active-NPC (ANPC), this connection is carried out by power switches. In addition, the clamping diodes are not immune to failure. When an open-circuit fault occurs in a clamping diode, the output current and voltage

distortion increase. In addition, the DC link capacitor voltages would differ significantly from the nominal value, which leads the capacitors to breakdown. Hence, identifying the defective clamping diode and subsequently applying an appropriate fault-tolerant strategy is mandatory to suppress the previously mentioned consequences and ensure service continuity in the nominal mode. However, in most of the research studies, identifying a faulty clamping diode and ensuring the service continuity in case of breakdown are overlooked. In the majority of the research efforts dealing with fault diagnosis and fault-tolerant operation in NPC inverters, the identification approaches mainly concern the power switches, and they are based on the hypothesis that clamping diodes never break down. Thus, when an open-circuit fault appears in a clamping diode, erroneous fault detection and subsequently erroneous remedial actions are applied, according to the published open-circuit switch fault diagnosis algorithms, or the fault detection cannot be carried out. Consequently, the system operates under fault condition without remedial operation. Furthermore, these proposed diagnosis methods cannot be developed and generalized to provide fault diagnosis and appropriate service continuity when a clamping diode breaks down. In this regard, ensuring the fault-tolerant operation in the case of open-circuit failure in a clamping diode is rarely investigated, but it is of considerable importance. Previous research work is mainly classified into two categories. The work in the first category solely proposes the remedial operation subsequent to the fault diagnosis.



(a)



(b)

Figure 1. Scheme of (a) a three-phase five-level NPC/H-bridge inverter and (b) a single-phase five-level NPC inverter.

The studies included in the second category only propose the fault diagnosis method and do not deal with fault-tolerant operation. It should be noted that there are a few of papers that treat fault diagnosis and fault-tolerant operation together.

Regarding the first category, the research work presented in [4–7] proposes a switch fault-tolerant approach for three-level NPC converters, but these strategies are not able to guarantee continuity of service when a clamping diode is faulty. More particularly, in the research work presented in [1,8], the authors investigated the continuity of service of an NPC inverter. However, the proposed approach to ensure the continuity of service when a clamping diode breaks down was not studied. In [9], an open-circuit fault-tolerant approach for an NPC inverter is also examined. The strategy ensures the service continuity of the inverter when a clamping diode is faulty (open circuit). In this paper, in order to generate the desired voltage level at the terminal of the inverter, the infeasible switching states are replaced by the possible ones, and the dwell time of the switching states is changed. Nevertheless, service continuity is performed in degraded mode, by applying two-level switching instead of three-level switching. Consequently, the total harmonic distortion of the output current is increased, compared with those in healthy operation. In [10], under clamping diode failure, the service continuity of an NPC inverter is accomplished without redundant components. In the case of fault occurrence, by utilizing the inherent characteristics of the three-level NPC inverter, the impossible control orders are replaced with the available ones. After remedial actions, the inverter is not able to deliver the rated power because the desired voltage amplitude cannot be generated at the terminal. In [11], authors studied remedial actions when a clamping diode is faulty (open circuit). Without employing any redundant leg, the rated terminal voltage is generated using inherent redundancy of the inverter, but the total harmonic distortion of the output voltage and output current is increased.

Concerning the second category, the research work presented in [12–18] deals with switch fault diagnosis in NPC inverters but cannot locate an open-circuit fault in a clamping diode. In [12], according to the Average Current Park's Vector, the faulty phase can be identified. However, the faulty switch and the defective clamping diode cannot be identified by this approach. By employing average Current Park's Vector strategy in [13], the faulty switch is pinpointed in a three-phase NPC circuit, but this presented approach cannot locate a defective clamping diode. In [14], in accordance with the current patterns resulting from an open-switch fault event in a three-phase NPC inverter and the duration of zero current, a faulty switch can be located. The defective clamping diode cannot be identified. The approach presented in [15] is only able to identify the defective phase in a three-phase NPC inverter. In addition, pole voltage measurement is carried out using additional sensors and circuits. The approach proposed in [16] can identify a defective switch by comparing the measured pole voltage and estimated pole voltage for a three-phase NPC rectifier. Moreover, this method cannot identify the defective clamping diode.

The authors of [19] present a fault diagnosis strategy that necessitates employing three extra sensors to measure the pole voltages to pinpoint a defective clamping diode in an NPC inverter. In [9], based on the analysis carried out on the distorted current resulting from a faulty clamping diode (open circuit) in NPC converters, the defective phase is determined. Then, by injecting the under-excited current, the faulty diode is pinpointed. In the particular case of a single-phase NPC/H-bridge converter [20], the authors proposed an approach based on the estimation of the grid current. Then, in all possible cases for open-circuit failures in clamping diodes, the fault diagnosis is accomplished by analyzing the generated residual value. Here, the grid parameters such as the transformer inductance and resistance are required. In [21], a clamping diode fault diagnosis is carried out by analyzing the electromagnetic emissions. This method requires external antennas and filters.

This paper comprises two major parts concerning a single-phase five-level NPC inverter. The first one deals with the fault diagnosis to finally perform fault-tolerant operation. The second part presents the remedial actions. The proposed diagnosis approach encompasses several superiorities compared to the research studies mentioned in the literature.

For fault diagnosis, employing extra sensors and hardware and complicated calculations and modeling is avoided. Moreover, the proposed diagnosis method does not rely on the load or grid parameters. Moreover, it can be implemented on field-programmable gate array (FPGA), and high time performances can be obtained. Furthermore, the proposed fault detection method is not affected by system imperfections and measurement errors. Above all, the faulty clamping diode can be identified fast and efficiently, which is seldom seen in past research work. The second section concentrates on the fault-tolerant operation when an open-circuit fault occurs in a clamping diode. The presented approach offers several paramount advantages. To realize the remedial operation, no additional components or bidirectional switches are utilized. Moreover, the nominal power can be delivered during the fault-tolerant operation, and the output current and output voltage are not changed or deteriorated in terms of distortion after remedial actions.

In Section 2, we introduce the fault diagnosis approach we propose. In the third section, the continuity of service is detailed. In Section 4, we present and discuss the simulation results. Selected experimental results are provided and discussed in Section 5. Finally, in the last section, we conclude this paper.

2. Principle of the Clamping Diode Fault Diagnosis Approach

Prior to remedial actions, the faulty component has to be identified. The fault diagnosis approach is constituted of two stages. In stage one, the fault occurrence is detected. In the second stage, called fault localization, following fault detection, the defective component is pinpointed. The scheme of the studied NPC circuit is depicted in Figure 1b. The conducting components during each switching state and the corresponding control orders are tabulated in Tables 1 and 2, respectively.

Table 1. Passing components corresponding to each switching state for positive and negative output currents in healthy operation.

Switching State	Terminal Voltage	Conducting Components ($I > 0$)	Conducting Components ($I < 0$)
1	+Vdc	S11, S12, S23, S24	D11, D12, D23, D24
2	+Vdc/2	S11, S12, S23, DC4	D11, D12, S22, DC3
3	+Vdc/2	DC1, S12, S23, S24	DC2, S13, D23, D24
4	0	S11, S12, D22, D21	D11, D12, S21, S22
5	0	DC1, S12, S23, DC4	DC2, S13, S22, DC3
6	0	D14, D13, S23, S24	S13, S14, D24, D23
7	−Vdc/2	DC1, S12, D22, D21	DC2, S13, S22, S21
8	−Vdc/2	D14, D13, S23, DC4	S13, S14, DC3, S22
9	−Vdc	D14, D13, D22, D21	S13, S14, S22, S21

Table 2. Switching patterns corresponding to each voltage level.

Switching State	Terminal Voltage	S11	S12	S13	S14	S21	S22	S23	S24	Attributed Decimal Number
1	+Vdc	1	1	0	0	0	0	1	1	195
2	+Vdc/2	1	1	0	0	0	1	1	0	198
3	+Vdc/2	0	1	1	0	0	0	1	1	99
4	0	1	1	0	0	1	1	0	0	204
5	0	0	1	1	0	0	1	1	0	102
6	0	0	0	1	1	0	0	1	1	51
7	−Vdc/2	0	1	1	0	1	1	0	0	108
8	−Vdc/2	0	0	1	1	0	1	1	0	54
9	−Vdc	0	0	1	1	1	1	0	0	60

2.1. Fault Detection Strategy

The fault detection approach relies on the measured and estimated output voltage. Based on the value of the DC link voltage and the applied control orders, the output voltage value is estimated. In more detail, as illustrated in Figure 2, the fault detection phase includes two parts. The first part deals with the voltage quantification. Even in healthy operation, the measured and estimated output voltage values are different, due to the measurement errors and voltage drop across the conducting components and the terminal current.

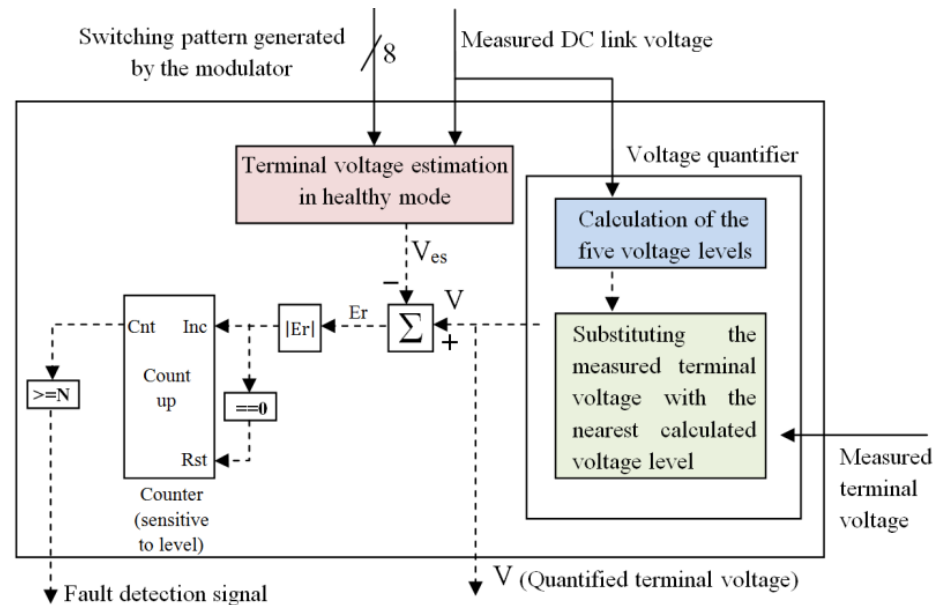


Figure 2. Proposed fault detection principle.

The five possible terminal voltage levels are calculated from the DC link voltage value. Then, the voltage quantifier assigns the nearest calculated voltage level to the measured terminal voltage, whose value is replaced by the quantified voltage, calculated from the same DC link voltage value (see Figure 2) used for output voltage estimation. In this way, false fault detection due to the above-mentioned errors is avoided. By means of the voltage quantifier, in contrast to [22], an accurate estimation of this voltage error is not needed. The second part is the counter. Because of the dead times and delays around the switching instants, the measured and estimated terminal voltage values are different. If this difference subsists beyond a certain time value (upper limit time of the counter called N_{max}), it means that this difference arises from a fault event. Otherwise, this difference is caused by the dead times and delays. The upper limit time of the counter (N_{max}) is fixed according to the total delay times of the components presented by the manufacturer, which is set at 20 μs in this study.

2.2. Fault Localization Strategy

Following fault detection, the clamping diode fault localization begins. We propose to use a failure mode analysis for the fault localization strategy. Applying this method allows us to locate a defective clamping diode by considering that the fault either occurred in a clamping diode or in a power switch. In this regard, Tables 3 and 4 gather all the cases of open-circuit faults in all components. Since the studied structure is symmetric, the fault localization is solely explained when the output current is positive.

Table 3. Identification of the defective component for positive current.

State	Faulty Switch or Diode	Conducting Components (Terminal Voltage)	Second Step	Conducting Components (Terminal Voltage)
1	S11	DC1, S12, S23, S24 (Vdc/2)	S24 is switched off	DC1, S12, S23, DC4 (0)
1	S24	S11, S12, S23, DC4 (Vdc/2)		S11, S12, S23, DC4 (Vdc/2)
1	S12	D14, D13, S23, S24 (0)	S23 is switched off	D14, D13, D22, D21 (−Vdc)
1	S23	S11, S12, D22, D21 (0)		S11, S12, D22, D21 (0)
2	S12	D14, D13, S23, DC4 (−Vdc/2)	S12 is identified in the first step.	
2	S11	DC1, S12, S23, DC4 (0)	S24 is switched on	DC1, S12, S23, S24 (Vdc/2)
2	S23	S11, S12, D22, D21 (0)		S11, S12, D22, D21 (0)
2	DC4	S11, S12, D22, D21 (0)		S11, S12, S23, S24 (Vdc)
3	S23	DC1, S12, D22, D21 (−Vdc/2)	S23 is identified in the first step.	
3	S12	D14, D13, S23, S24 (0)	S11 is switched on	D14, D13, S23, S24 (0)
3	DC1	D14, D13, S23, S24 (0)		S11, S12, S23, S24 (Vdc)
3	S24	DC1, S12, S23, DC4 (0)		S11, S12, S23, DC4 (Vdc/2)
5	S12	D14, D13, S23, DC4 (−Vdc/2)	S11 is switched on	D14, D13, S23, DC4 (−Vdc/2)
5	DC1	D14, D13, S23, DC4 (−Vdc/2)		S11, S12, S23, DC4 (Vdc/2)
5	S23	DC1, S12, D22, D21 (−Vdc/2)		S11, S12, D22, D21 (0) (see Table 5 for third step)
5	DC4	DC1, S12, D22, D21 (−Vdc/2)	S11, S12, D22, D21 (0) (see Table 5 for third step)	
7	S12	D14, D13, D22, D21 (−Vdc)	S11 is switched on	D14, D13, D22, D21 (−Vdc)
7	DC1	D14, D13, D22, D21 (−Vdc)		S11, S12, D22, D21 (0)
8	S23	D14, D13, D22, D21 (−Vdc)	S24 is switched on	D14, D13, D22, D21 (−Vdc)
8	DC4	D14, D13, D22, D21 (−Vdc)		D14, D13, S23, S24 (0)

Table 4. Identification of the defective component in the third step.

State	Faulty Switch or Diode	Third Step	Conducting Components (Terminal Voltage)
5, (I > 0)	S23	S24 is switched on	S11, S12, D22, D21 (0)
5, (I > 0)	DC4		S11, S12, S23, S24 (Vdc)
5, (I < 0)	S22	S21 is switched on	S13, S14, D23, D24 (0)
5, (I < 0)	DC3		S13, S14, S21, S22 (−Vdc)

Table 5. Modification of the switching states to acquire fault-tolerant operation.

Faulty Clamping Diode	Infeasible Switching State	Substituted Switching State
DC1	3	2
	5	4 or 6
	7	8
DC2	3	2
	5	4 or 6
	7	8
DC3	2	3
	5	4 or 6
	8	7
DC4	2	3
	5	4 or 6
	8	7

The failure mode analysis, allowing for the identification of a faulty component, is summarized in Tables 3 and 4. The third column (from left) in Table 3 is obtained by supposing an open-circuit fault in each component for all the switching states. The presented topology includes four clamping diodes (DC1, DC2, DC3, and DC4), four external switches (S11, S14, S21, and S24), and four internal switches (S12, S13, S22, and S23). If an open-circuit fault event occurs in the external switches, the clamping diode located in the same half-leg forms the current path rather than the defective external switch. If an open-circuit failure occurs in the internal switches or in the clamping diodes, the output current flows through the two antiparallel diodes situated in the opposite half-leg instead of the faulty internal switch or the defective clamping diode. In this way, the third column (from left) is obtained for all switching states and components forming the current path corresponding to each switching state. According to the last applied control orders, the quantified output voltage is compared with the estimated voltages presented in the third column (from left). Thus, the faulty component is identified. If the quantified terminal voltage is equal to more than one estimated voltage, the faulty component is not identified distinctly. Thus, it is mandatory to perform the next step. In the second step, the switching state is modified, and the new components forming the current path accompanying the corresponding terminal voltages are indicated in the fifth column (from left) of Table 3. Once again, the quantified terminal voltage is compared with the estimated voltages. Similar to the previous step, if necessary, the third step should be carried out. The results obtained after performing the third step are provided in Table 4. According to Tables 3 and 4, in order to identify the defective clamping diode, performing two or three steps is needed. In the simulation section, by giving an example, the applied fault localization strategy is clarified.

3. Principle of the Proposed Fault-Tolerant Strategy

In the following subsections, the modification of the switching states to be performed to realize the continuity of service is explained.

3.1. Open-Circuit Fault in DC1 or DC2

Based on Table 1, in switching states 3, 5, and 7, the output current flows through DC1 (positive current) or DC2 (negative current). Thus, if an open-circuit fault occurs in DC1 or DC2, the expected terminal voltages corresponding to switching states 3, 5, and 7 are not achievable. In this regard, as represented in Table 5, switching state 3 is substituted by switching state 2 to attain the terminal $+V_{dc}/2$. As shown in Table 1, in switching state 2 (regardless of the sign of the output current), the output current does not pass through DC1 or DC2. Hence, the terminal voltage can attain $+V_{dc}/2$, as desired. Switching state 5 can be substituted by switching state 4 or switching state 6 in which no clamping diode conducts the output current. We mentioned here that switching states 4 and 6 have a similar impact on the voltages of the neutral point and the DC link capacitors because in switching state 4 or switching state 6 (see Table 1) there is no current injected to the neutral point. Therefore, 0 V is made at the terminal either by substituting switching state 4 or switching state 6. In order to obtain an output voltage equal to $-V_{dc}/2$, switching state 7 is replaced by switching state 8. As mentioned in Table 5, in switching state 8, the terminal current does not pass through the clamping diodes DC1 or DC2.

3.2. Open-Circuit Fault in DC3 or DC4

As shown in the preceding subsection, Table 5 is established corresponding to the faulty clamping diodes DC3 or DC4. In case of fault occurrence in DC3 or DC4, the switching states 2, 5, and 8 are replaced by the switching states 3, 4 or 6, and 7, respectively. It should be noticed that in case of open-circuit failure in DC3 or DC4, switching state 4 or switching state 6 can be applied interchangeably because no current flows into the neutral point in both cases.

4. Simulation Results

Some selected simulation results are represented in the following. First, fault diagnosis is discussed. In the second subsection, some results about the applied fault-tolerant strategy are elaborated. Since the topology of the converter is symmetric, clamping diode DC4 was chosen as the faulty component. The simulation parameters are summarized in Table 6.

Table 6. Simulation parameters associated with their values.

Parameters	Values
Load resistance	27.7 Ω
Load inductance	9 mH
DC link voltage	50 V
DC link capacitor	2.2 mF
Switching frequency	1 kHz
Modulation index	0.8

4.1. Fault Diagnosis Strategy

Depending on the last applied switching state in healthy conditions, the faulty component can be identified in the first, second, or third steps (Tables 3 and 4). In order to avoid presenting similar results, we chose to detail the most complicated case study. In this regard, DC4 was considered as the faulty component. In Figure 3, we present the fault localization procedure for the clamping diode DC4. In order to better represent the defective component in the simulations, we attributed decimal numbers to the power switches and clamping diodes. We attributed to S11, S12, S13, S14, S21, S22, S23, S24, DC1, DC2, DC3, and DC4, the numbers 128, 64, 32, 16, 8, 4, 2, 1, 3, 9, 27, and 81, respectively. As represented in Figure 3, before instant t_1 (interval 1), the converter is in normal operation, and the output voltage and switching state attain 0 V and 102 (switching state 5). Hence, right before the failure in DC4 (instant t_1), the current chooses DC1, S12, S23, and DC4. As the generated open-circuit fault occurs in DC4 at instant t_1 , the quantified voltage takes $-V_{dc}/2$, in accordance with Table 3. Then, the fault is detected at instant t_2 . However, the localization of the defective component is still not possible because in accordance with Table 3, in cases where an open-circuit fault occurs in S12, DC1, S23, or DC4, the same quantified voltage $-V_{dc}/2$ results at the first step. Therefore, the execution of the second step is required in which the power switch S11 is turned on once the fault detection signal is generated at instant t_2 as can be seen in Figure 3. Once S11 conducts, the current path in accordance with Table 3 is constituted by S11, S12, D22, and D11. Hence, the quantified voltage attains 0 at instant t_3 because of the dead time of the drivers (interval 3). Based on the corresponding subsection in Table 3, after the first modification of the switching pattern (the second step), the quantified terminal voltages resulted by open-circuit fault occurrence in S23 and DC4 are the same and equal to 0 V.

Thus, it is not possible to determine the defective component (between S23 and DC4) after performing the second step. Thus, performing the third step is indispensable. To this end, according to Figure 3, at instant t_4 , the third step S24 is switched on. After passing interval 5, the quantified terminal voltage is equal to $+V_{dc}$ at instant t_5 . Based on the failure-mode analysis summarized in Table 4, the defective diode DC4 is pinpointed at instant t_6 .

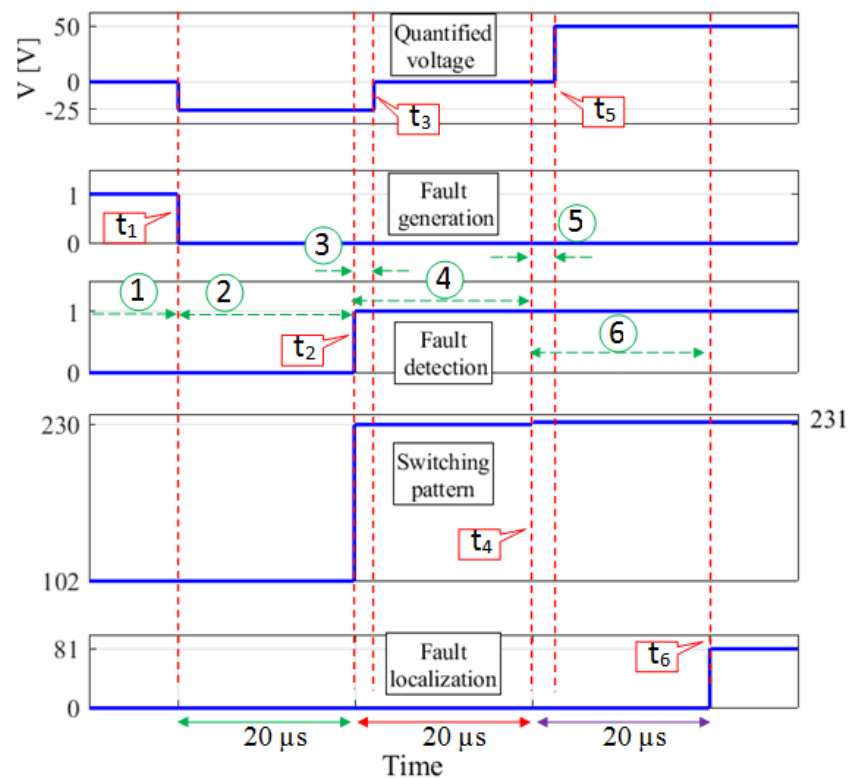


Figure 3. Simulation results for localization of faulty clamping diode DC4 in the third step.

4.2. Fault-Tolerant Strategy

Subsequent to the identification of the defective clamping diode explained in the previous subsection, remedial operation of the inverter begins. To perform continuity of service, we used an approach that does not require any additional or redundant components. Solely by modification of certain switching states (used in healthy conditions—see Table 5), service continuity is ensured. Figure 4 illustrates the case of an open-circuit failure in DC4, without applying a fault-tolerant strategy. One can notice that the two DC link capacitor voltages start to differ from their nominal values, and the output voltage and current are deteriorated in terms of distortion. In the case of the fault event in DC4, the proposed remedial actions are illustrated in Figures 5 and 6. It should be noted that in Figures 5 and 6, the interval between the fault occurrence and the triggering of the fault tolerant operation (faulty component identification) is not visible because according to the results presented in Figure 3, this interval lasts 60 μs, which is not large enough to be seen in Figures 5 and 6. As shown in Figure 5, during post-fault operation, the output voltage and current are the same as those during healthy operation. Moreover, despite low-frequency oscillation with negligible ripple amplitude in the DC link capacitor voltages, the neutral point voltage is stabilized. In Figure 6, the modifications of the switching states are represented.

In this respect, the switching states corresponding to the same output voltage levels during healthy operation and fault-tolerant operation are compared. In Figure 6, the gate signals G11, G12, G23, and G24 represent the applied switching state. The other gate signals are complementary to the selected ones. Hence, according to the aforementioned gate signals, the corresponding switching state can be obtained. During healthy operation (interval a_1), the output voltage levels +Vdc and +Vdc/2 are made. By referring to Table 2, switching states 1, 2, and 3 are applied in this interval. During interval a_2 , the same output voltage levels (+Vdc and +Vdc/2) are obtained compared with interval a_1 , but the switching state 2 is substituted with switching state 3. Indeed, over the entire interval a_2 , G12, G23, and G24 are set at '1', and only G11 is toggled between '0' and '1', which complies with Table 5. In accordance with the data summarized in Table 2, switching states 1, 2, and 3 are applied during this interval. In accordance with the output voltage levels acquired during

interval b_1 ($-V_{dc}$ and $-V_{dc}/2$) and by referring to Table 2, one can deduce that switching states 7, 8, and 9 are applied in this interval. By comparing the gate signals applied in interval b_2 (fault-tolerant operation) with those applied in interval b_1 , it is deduced that state 8 is substituted by state 7 (G11, G23, and G24 are set at '0', and G12 is toggled between '0' and '1'). Likewise, one can notice that switching states 2 and 5 are substituted with switching states 3 and 4, respectively.

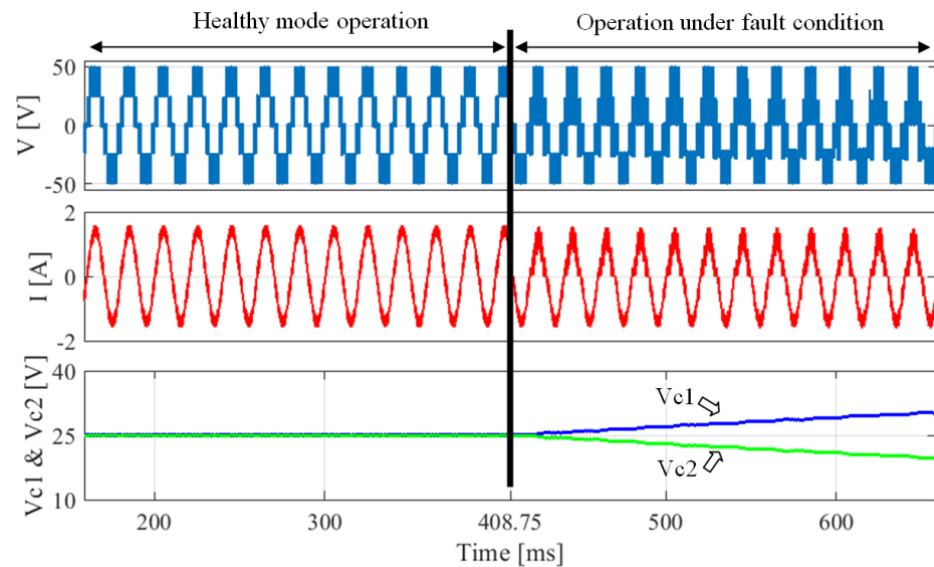


Figure 4. Simulation results of the inverter operation under open-circuit fault occurrence in DC4, without fault-tolerant control.

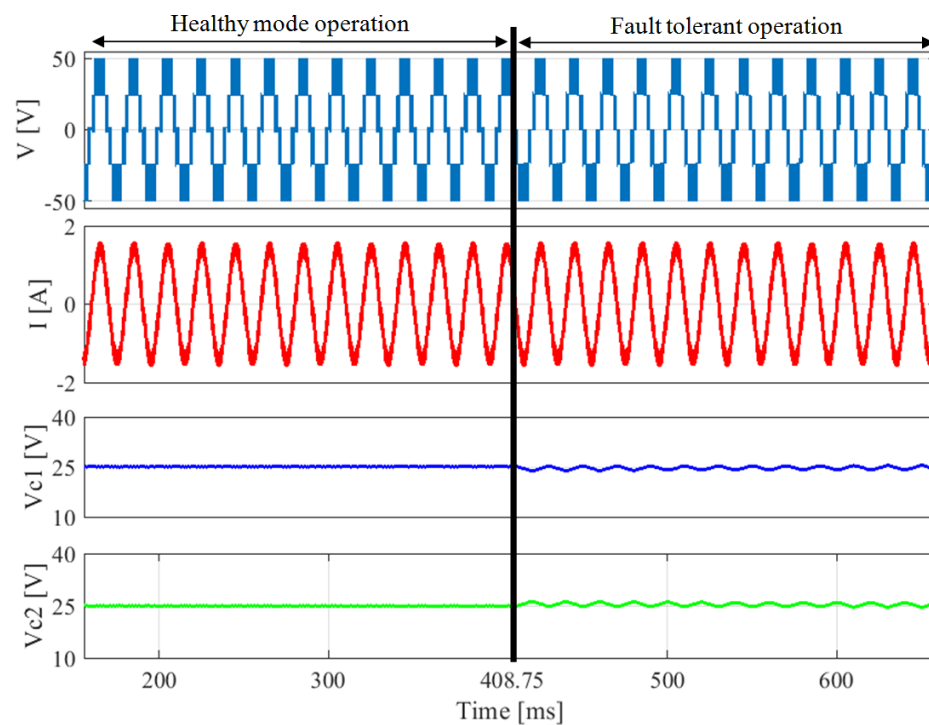


Figure 5. Simulation results for fault-tolerant operation of the inverter in case of fault occurrence in DC4.

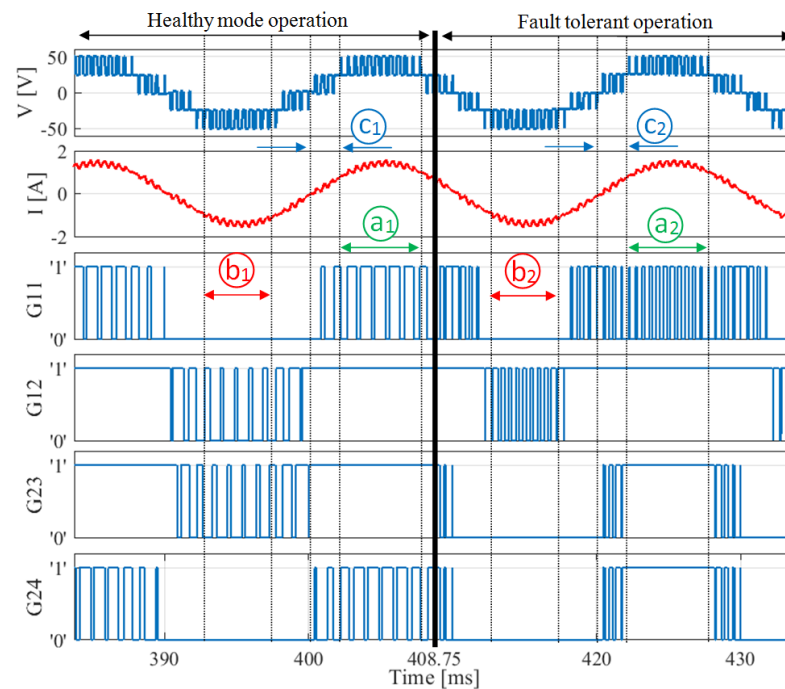


Figure 6. Detailed representation of the fault-tolerant operation in case of open-circuit fault occurrence in DC4.

5. Experimental Results

To implement the presented algorithms and approaches, a dSPACE platform (MicroLabBox) including a Xilinx FPGA chip was employed. Since the fault diagnosis and modifications of the switching states during post-fault operation should be performed quickly, these operations were implemented on the FPGA module of the dSPACE. The employed converter comprises IGBTs with the reference number of SKM50GB123D (fabricated by SEMIKRON), commanded by SKHI22A drivers. The test bench employed is given in Figure 7. The same parameters pointed out in the simulation subsection were used on the employed test bench.

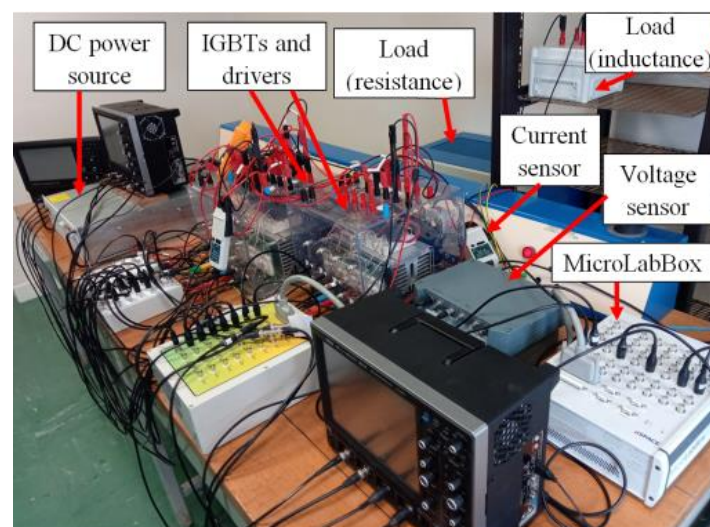


Figure 7. Experimental test bench.

To create the failure in the clamping diodes, an auxiliary IGBT was used. To generate the open-circuit fault in the clamping diode, the auxiliary IGBT, connected in series with the relevant clamping diode and constantly closed in healthy conditions, was switched off.

In the experimental results, the four gate signals applied to the power switches represent the switching pattern. In accordance with Table 2 and the four represented gate signals and based on the fact that the other four gate signals are complementary, each switching state can be estimated. Moreover, similar to the simulation section, clamping diode DC4 was considered as the faulty component.

In Figure 8, before the fault occurrence in DC4, the converter is in healthy conditions (interval 1). In this case, switching state 2 is applied, and the output voltage attains $+V_{dc}/2$ (in accordance with Table 2), and after the instant t_a , the applied switching state and the output voltage are 5 and 0 V, respectively. The open-circuit failure is created in DC4 at the instant t_b , and then the output voltage attains $-V_{dc}/2$. At t_c , the counter starts and reaches the upper limit value. The failure is detected at t_d , but it is still not possible to identify the faulty component among S12, DC1, S23, and DC4. Thus, the second step is necessary, by switching on S11 according to Table 3. Thus, S11 is switched on at instant t_d , and the output voltage takes 0 V. However, after the execution of the second step, the defective component is still not distinguished between components S23 and DC4. Thus, performing the third step is necessary. For this purpose, at instant t_e , S24 is switched on, and the output voltage reaches $+V_{dc}$. Hence, at instant t_f , DC4 is located as faulty. It should be mentioned that intervals 3 and 4 are considered to avoid any misdiagnosis because of dead times, delays, and transition times. The experimental results regarding the fault tolerant operation are represented in Figures 9–11. Since the results presented in Figures 9–11 are almost identical to Figures 4–6, respectively, any repetitive explanation is avoided in this section. The detailed analysis and explanations are presented and discussed earlier.

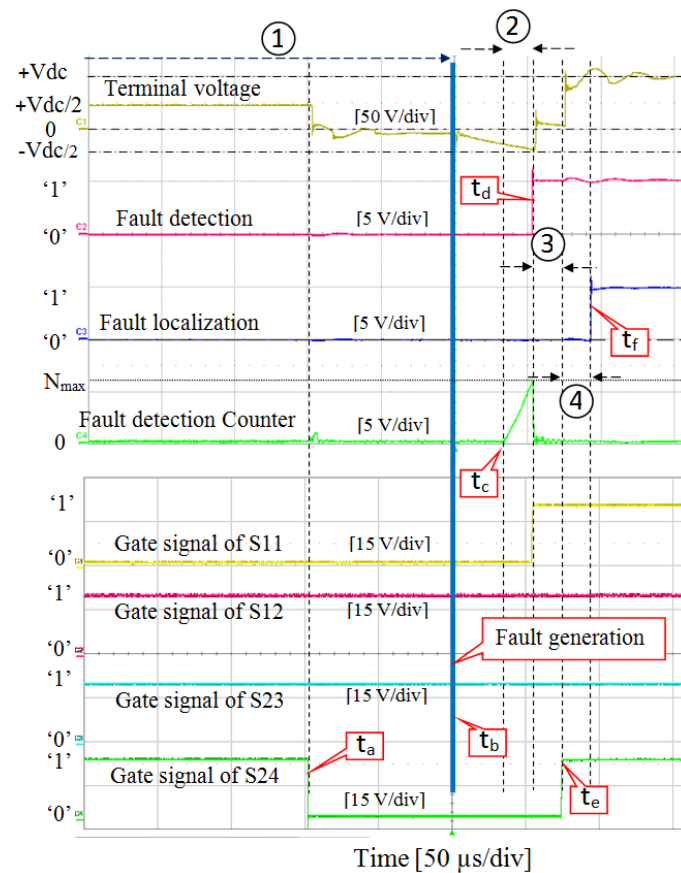


Figure 8. Experimental results for localization of faulty clamping diode DC4 in the third step.

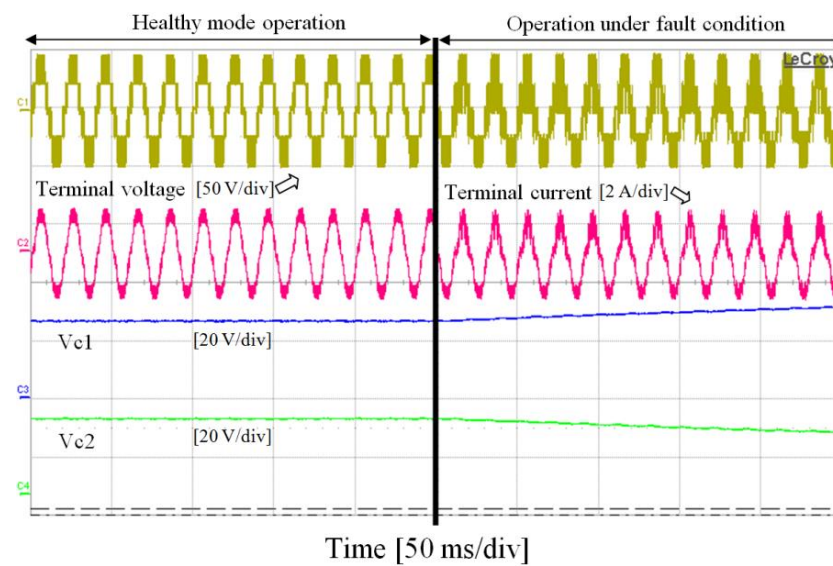


Figure 9. Experimental results of the inverter operation under fault condition without fault-tolerant control.

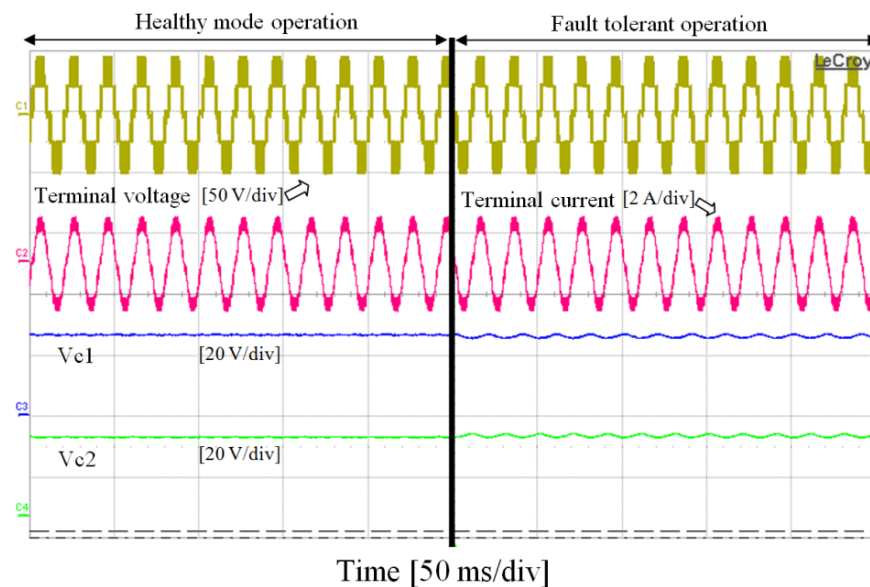


Figure 10. Experimental results of the inverter operation with fault-tolerant control.

It is important to mention that the case of a faulty clamping diode has been rarely studied in the literature; most of the time, it is assumed that these diodes never break down. Compared with the literature, this work proposes an original contribution to perform the continuity of service of five-level neutral-point-clamped inverters under clamping diode open-circuit failure, concerning two main aspects. First, regarding the fault diagnosis (detection and localization), we propose a logic-based method that does not require extra sensors or complicated calculations or modeling. Secondly, to perform fault-tolerant operation, no additional components are required, and the post-fault operation is realized at rated power, with the terminal current and voltage being the same before and after the fault occurrence. Table 7 summarizes the drawbacks of the conducted research compared with our contribution.

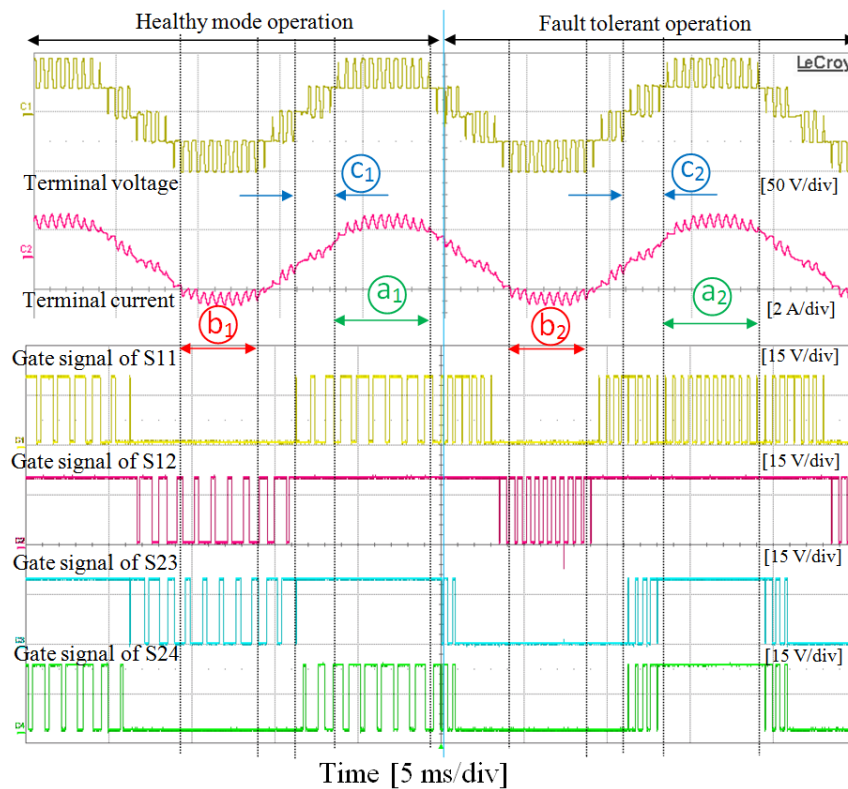


Figure 11. Detailed experimental results of the fault-tolerant strategy.

Table 7. Drawbacks of the conducted research work compared with this paper.

References	Drawback
[1,4–8]	Are not able to ensure fault-tolerant operation in case of fault event in a clamping diode
[9,11]	Output voltage THD increases during post-fault operation
[10]	The rated voltage is not restored during post-fault operation
[12,18]	Are not able to locate a defective clamping diode
[19]	Extra sensors are required for fault diagnosis
[20]	Knowing the grid parameters is required for fault diagnosis
[21]	External antennas and filters are required for fault diagnosis

6. Conclusions

We have proposed a fast and efficient fault-tolerant method for clamping diodes of five-level NPC inverters. The fault diagnosis step does not require complicated calculations. Thus, it can be implemented on FPGA to achieve a high time performance. Moreover, it does not require any additional sensor, hardware, or component modeling. The diagnosis method is able to identify the faulty clamping diode. Following the fault diagnosis, this paper focuses on ensuring the continuity of service of the inverter in case of fault occurrence in clamping diodes. Secondly, the fault event in clamping diodes can cause the DC link capacitors to breakdown, and the fault event deteriorates the harmonic content of the terminal voltage and current. The proposed fault-tolerant approach is also realized without employing any redundant or additional components. Furthermore, during the post-fault operation, the rated current and voltage are achieved at the terminal. The simulation and experimental results are reported to validate the proposed strategy. As mentioned above, this paper presented fault diagnosis and fault-tolerant operation under an open-circuit fault event in clamping diodes, which has been rarely investigated. In summary, the proposed strategy can be applied in practice where an open-circuit fault occurs in a clamping diode, which is rarely taken into consideration in the already conducted research work.

Author Contributions: Investigation: S.A., P.P. and S.S.; Methodology: S.A., P.P. and S.S.; Supervision: P.P., S.S., and D.A.K.; Writing—original draft: S.A.; Writing—review and editing: P.P., D.A.K. and S.S. All authors have read and agreed to the published version of the manuscript.

Funding: This research work is the result of the collaboration between the University of Lorraine (France) and Iran University of Science and Technology (IUST) started in October 2018. It has been partially financially supported by the Scientific and Technologique Cooperation Service of the French Embassy in Tehran, and for this we express our thanks.

Conflicts of Interest: The authors declare no conflict of interest.

References

1. Gautam, S.P.; Kumar, L.; Gupta, S.; Agrawal, N. A single-phase five-level inverter topology with switch fault-tolerance capabilities. *IEEE Trans. Ind. Electron.* **2017**, *64*, 2004–2014. [\[CrossRef\]](#)
2. Rodriguez, J.; Lai, J.S.; Peng, F.Z. Multilevel inverters: A survey of topologies, controls, and applications. *IEEE Trans. Ind. Electron.* **2002**, *49*, 724–738. [\[CrossRef\]](#)
3. Wu, B. *High-Power Converters AC Drives*; Wiley: Hoboken, NJ, USA, 2006.
4. Lee, J.; Lee, K. Open-switch fault tolerance control for three-level NPC/T-Type rectifier in wind turbine systems. *IEEE Trans. Ind. Electron.* **2015**, *62*, 1012–1021. [\[CrossRef\]](#)
5. Lee, J.; Lee, K. Open-circuit fault-tolerant control for outer switches of three-level rectifier in wind turbine systems. *IEEE Trans. Power Electron.* **2016**, *31*, 3806–3815. [\[CrossRef\]](#)
6. Ceballos, S.; Pou, J.; Zaragoza, J.; Robles, E.; Villate, J.L.; Martin, J.L. Fault-tolerant neutral-point-clamped converter solutions based on including a fourth resonant leg. *IEEE Trans. Ind. Electron.* **2011**, *58*, 2293–2303. [\[CrossRef\]](#)
7. Ceballos, S.; Pou, J.; Robles, E.; Gabiola, I.; Zaragoza, J.; Villate, J.L.; Boroyevich, D. Three-level converter topologies with switch breakdown fault-tolerance capability. *IEEE Trans. Ind. Electron.* **2008**, *55*, 982–995. [\[CrossRef\]](#)
8. Rao, M.; Sivakumar, K. A fault-tolerant single phase five-level inverter for grid independent PV systems. *IEEE Trans. Ind. Electron.* **2015**, *62*, 7569–7577.
9. Choi, U.; Lee, J.; Blaabjerge, F.; Lee, K. Open-circuit fault diagnosis and fault-tolerant control for a grid-connected npc inverter. *IEEE Trans. Power Electron.* **2016**, *31*, 7234–7247. [\[CrossRef\]](#)
10. Li, S.; Xu, L. Strategies of fault tolerant operation for three-level PWM inverters. *IEEE Trans. Power Electron.* **2006**, *21*, 933–940. [\[CrossRef\]](#)
11. Ceballos, S.; Pou, J.; Robles, E.; Zaragoza, J.; Martin, J.L. Performance evaluation of fault-tolerant neutral-point-clamped converters. *IEEE Trans. Ind. Electron.* **2010**, *57*, 2709–2718. [\[CrossRef\]](#)
12. Abadi, M.B.; Mendes, A.M.S.; Cruz, S.M.A. Three-level NPC inverter fault diagnosis by the average current Park's vector approach. In Proceedings of the 20th ICEM, Marseille, France, 2–5 September 2012; pp. 1893–1898.
13. Mendes, A.M.S.; Abadi, M.B.; Cruz, S.M.A. Fault diagnosis algorithm for three-level neutral point clamped AC motor drives based on average current Park's vector. *IET Power Electron.* **2014**, *7*, 1127–1137. [\[CrossRef\]](#)
14. Lee, J.S.; Lee, K.B.; Blaabjerg, F. Open-switch fault detection method of a back-to-back converter using NPC topology for wind turbine systems. *IEEE Trans. Ind. Appl.* **2015**, *50*, 325–335. [\[CrossRef\]](#)
15. Kim, T.J.; Lee, W.C.; Hyun, D.S. Detection method for open circuit fault in neutral-point-clamped inverter systems. *IEEE Trans. Ind. Electron.* **2009**, *56*, 2754–2763.
16. Caseiro, L.M.A.; Mendes, A.M.S. Real-time IGBT open-circuit fault diagnosis in three-level neutral-point-clamped voltage-source rectifiers based on instant voltage error. *IEEE Trans. Ind. Electron.* **2015**, *62*, 1669–1678. [\[CrossRef\]](#)
17. Choi, U.M.; Jeong, H.G.; Lee, K.B.; Blaabjerg, F. Method for detecting an open-switch fault in a grid-connected NPC inverter system. *IEEE Trans. Power Electron.* **2012**, *27*, 2726–2739. [\[CrossRef\]](#)
18. Fazio, P.; Maragliano, G.; Marchesoni, M.; Parodi, G. A new fault detection method for NPC converters. In Proceedings of the 14th European Conference on Power Electronics and Applications, Birmingham, UK, 30 August–1 September 2011; pp. 1–10.
19. Mendes, A.M.S.; Abadi, M.B.; Cruz, S.M.A. Method to diagnose open-circuit faults in active power switches and clamp-diodes of three-level neutral-point clamped inverters. *IET Elect. Power Appl.* **2016**, *10*, 623–632.
20. Ge, X.; Pu, J.; Ge, B.; Liu, Y. An open-circuit fault diagnosis approach for single-phase three-level neutral-point-clamped converters. *IEEE Trans. Power Electron.* **2018**, *33*, 2559–2570. [\[CrossRef\]](#)
21. Abari, I.; Lahouar, A.; Hamouda, M.; Slama, J.B.H.; Al-Haddad, K. Fault detection methods for three-Level NPC inverter based on DC-bus electromagnetic signatures. *IEEE Trans. Ind. Electron.* **2018**, *65*, 5224–5236. [\[CrossRef\]](#)
22. Shahbazi, M.; Poure, P.; Saadate, S.; Zolghadri, M.R. Fault-tolerant five-level converter topology with FPGA-based reconfigurable control. *IEEE Trans. Ind. Electron.* **2013**, *60*, 2284–2294. [\[CrossRef\]](#)